Interaction of local anesthetics with phospholipids in Langmuir monolayers

Suzanne Amador Kane[1,*] and Samuel D. Floyd[2]
[1]*Physics Department, Haverford College, Haverford, Pennsylvania 19041*
[2]*Biology Department, Haverford College, Haverford, Pennsylvania 19041*
(Received 12 April 2000)

We have used epifluorescence microscopy to study the interactions of two local anesthetics of the ''caine'' family (tetracaine and dibucaine), with Langmuir monolayers of the phospholipid dipalmitoylphosphatidylcholine (DPPC). These results show that incorporation of either dibucaine or tetracaine causes significant changes in the domain shapes of the liquid condensed phase in monolayers. In particular, at low *p*H, where the charged cationic form of the local anesthetics predominates, local anesthetic: DPPC monolayers formed significantly less compact liquid condensed domains with highly ramified shapes, compared to DPPC-only controls. For high *p*H values at which both local anesthetics are electrically neutral, the liquid condensed domains in mixed monolayers resembled that of DPPC-only controls, indicating that these effects have their origins in electrostatic interactions between the local anesthetics and the phospholipid headgroups. Epifluorescence images obtained using the intrinsic fluorescence of dibucaine indicated that dibucaine partitions into both the liquid condensed and liquid expanded phases.

PACS number(s): 87.14.Cc, 87.16.Dg

INTRODUCTION

In spite of the long history of local anesthetic use, much remains unknown about the specific mechanisms by which local anesthetics of the ''caine'' family achieve their efficacy [1,2]. It is generally accepted that their anesthetic effect comes from an inhibition of the production of action potentials by sodium ion channels, and molecular mechanisms involved in this phenomenon are becoming clear [3–5]. The correlation which exists between local anesthetic (LA) potency and membrane solubility has led many authors to propose that these drugs' interesting pharmacological properties depend on their interactions with biological membranes, at least as an intermediate step to specific binding to a protein target [6–9]. Researchers have also investigated using lipid drug carriers as a more effective means of delivering LA's for procedures like epidural anesthesia or topical local anesthesia, and clinical studies have shown that encapsulation of the drugs in liposomes allows their timed release, and thus prolongs the duration of the anesthesia [10–14].

Several theories have been developed to explain the way the ''caine'' anesthetics—such as dibucaine and tetracaine (Fig. 1)—might modify the structure of biological membranes [7,9]. One line of thought holds that the anesthetic molecules are inserted into the membrane as a whole and ''fluidize'' it. While the nature of this ''fluidity'' has not been clearly defined, it has been hypothesized to relate to either a local expansion of the membrane, or to disordering of the phospholipids in the outer monolayer, either of which provides a modified membrane environment to integral membrane proteins. Alternatively, it has been suggested that LA molecules may localize in regions of relatively disordered phospholipid structure in the immediate vicinity of transmembrane proteins, and that this may account in part for their strong physiological effect even at low concentrations [15,16].

Dibucaine (DIB) and tetracaine (TTC) are known to insert into both bilayer and monolayer membrane systems [16–22]. The interactions of DIB and TTC with phospholipids are linked to their charge state, since both have an amine with a pK_a of approximately 8.0–8.5 in membranes; both molecules are protonated at low *p*H, and neutrally charged at high *p*H [17]. One mechanism by which DIB and TTC could modify the ordering of the phospholipids within biological membranes involves electrostatic interactions with the phospholipid headgroups [17,18,20,23,24]. For zwitterionic phospholipids, such as dipalmitoylphosphatidylcholine (DPPC), there exists the potential for electric dipole-dipole interactions. These have been hypothesized to occur between the protonated ammonium ion and lone-pair electrons of the butoxy group of DIB, and the PO_4^- and $N(CH_3)_3^+$ of DPPC's headgroup, respectively. A similar interaction also can take place between DPPC and the TTC electric dipole resulting from its cationic head and C═O group. This *attractive* interaction would disrupt the strong dipole-dipole repulsion between DPPC headgroups; this repulsion has been proposed as a dominant factor in determining DPPC monolayer phase behavior [25,26]. In addition, both DIB and TTC interact very differently with anionic than with zwitterionic phospho-

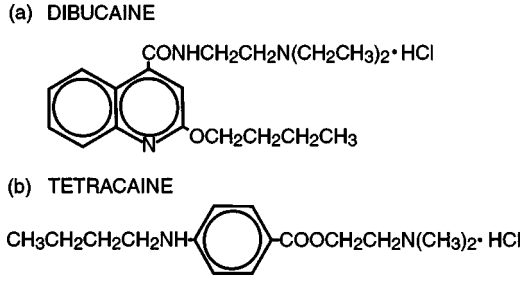

FIG. 1. Chemical structure of (a) dibucaine (DIB) and (b) tetracaine (TTC).

*Author to whom correspondence should be addressed.

lipids [18,27,28]. In either case, these electrostatic interactions should not exist at *p*H values well above the *p*Ka [20,23].

A related question involves how the LA molecules insert into the membrane. Nuclear Overhauser effect spectroscopy (NOESY) measurements on vesicles containing DIB and TTC have indicated that TTC probably inserts its hydrophobic chains into the bilayer, while DIB may only associate with the phospholipid's headgroups [17]. Other work provided support for the idea that TTC actually intercalates into the bilayer [21], while providing conflicting evidence on whether DIB incorporates in the same way [29]. Calorimetric studies were interpreted to mean that DIB in vesicles reduces the average size of gel-phase clusters, and leads to the growth of domains with ramified boundaries [19].

The interactions between LA's and phospholipids was studied in model membrane systems, including vesicles and micelles, using a variety of spectroscopic and calorimetric techniques [17–23,27,30]. Some studies investigated these systems using Langmuir monolayer methods to understand how these molecules affect phospholipid phase behavior [28,29], specifically by measuring the surface pressure-molecular area isotherms of phospholipid-LA monolayers and their electrical surface potential. However, these techniques only allow measurements to be made over the entire membrane or monolayer, and therefore allow only average effects to be observed. Epifluorescence microscopy, however, allows one to visualize the phase behavior of a monolayer system at length scales of micrometers. Thus the extent of uniformity in the distribution of the LA can be directly visualized. In addition, this technique permits the observation of the effect of the incorporation of LA's on domain formation as the membrane's phospholipids condense into more ordered phases. The work presented here shows how epifluorescence microscopy of monolayers of phospholipid-LA mixtures show the effects on in-plane ordering in two-dimensional analogs of the biologically relevant fluid-gel phases. These experiments could also give insight into applications which depend on phospholipid-drug interactions.

MATERIALS AND METHODS

All phospholipid samples were purchased from Avanti Polar Lipids (Alabaster, AL), and used without further purification. Dibucaine hydrochloride (99% purity) was purchased from Aldritch (Milwaukee, WI) and tetracaine hydrochloride (99% purity) was purchased from Sigma (St. Louis, MO). The LA: DPPC concentrations and temperature ranges used were chosen to agree with earlier studies of model systems. The fluorescent probe used was the acyl-chain labeled 2-[12-(7-nitrobenz-2-oxa-1,3-diazol-4-yl)amino]dodecanoyl-1-hexadecanoyl-*sn*-glycero-3-phosphocholine (NBD-PC) purchased from Avanti Polar Lipids. According to x-ray diffraction results, the phase traditionally called the liquid expanded (LE) or fluid phase corresponds to a two-dimensional fluid, with disordered hydrocarbon chains, while the liquid condensed (LC), or gel phase, has longer distance positional correlations, and long range bond orientational order possibly corresponding to a two-dimensional hexatic phase [31,32]. At molecular areas approaching close packing, the monolayer undergoes a further transition into the *S* phase, which likely corresponds to a two-dimensional crystal, with longer range positional order and ordered hydrocarbon chains [31,32] NBD-PC is known to accumulate preferentially in the LE phase relative to the LC phase in the LE-LC coexistence region, permitting direct visualization of the growth of LC and *S* domains. Probe concentrations of 1 mol % were used to label the lipid samples. Studies of isotherms for various probe concentrations were performed to establish that this probe concentration has a negligible effect on the monolayer behavior. All solvents used in the experiment were HPLC grade, and all chemicals used to prepare the subphase were highest grade ACS reagents, purchased from either Aldrich or Fisher Scientific (Fairlawn, NJ). Ultrapure Milli-*Q* water (Millipore Corporation, Bedford, MA) was used to prepare the subphase of 0.15-M NaCl titrated to 7.0 *p*H with HCl and NaOH. The data shown here for *p*H 6.0 were performed without buffer in the subphase, while all *p*H 9.5 data shown were taken with 50-mM boric acid buffer. However, all controls were reproduced for the *p*H 6.0 results using boric acid buffer in the subphase to confirm that its presence did not affect the low *p*H results. All samples were spread from a 2:1 v/v chloroform-methanol solution at lipid concentrations of 1 mg/ml. All phospholipid and lipid compositions are given as w/w ratios.

The Langmuir trough used was a KSV Instruments (Riv-

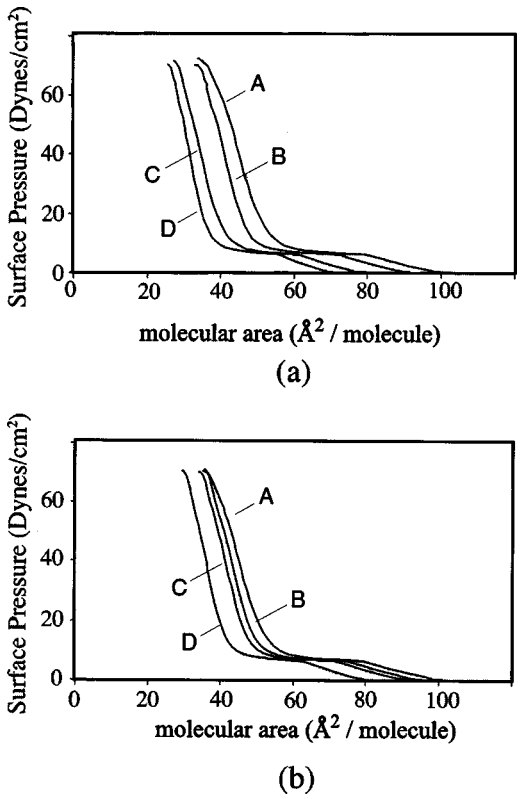

FIG. 2. Isotherms obtained for LA:DPPC monolayers containing varying concentrations of (a) DIB and (b) TTC. Isotherms are shown for (right to left) 0, 9, 16, and 25 mol %. In general, the overall shape of each isotherm remains unaltered when the values of the molecular area are rescaled by a constant factor to reflect the molecular area due only to the DPPC in each film; this reflects the relatively small effective molecular area due to either DIB or TTC in each film.

TABLE I. Summary of measurements on isotherms of $f = 0-25$ mol % local anesthetic in DPPC Langmuir monolayers. A_1 is the molecular area at which the LC-LE coexistence region begins, while A_2 is the molecular area at which the surface pressure is equal to 30 dyn/cm. (Unless noted, all data have uncertainties of approximately ± 2 Å^2.) The constancy of the ratio A_1/A_2 is one indication that the overall shape of the isotherms does not change significantly with increasing local anesthetic concentration. The average in-plane molecular area for the local anesthetic molecules were computed from these data, assuming that the local anesthetics are entirely incorporated into the monolayer, and that DPPC molecules have the same molecular area in the local anesthetic samples as in the 0-mol % controls. The values of $A_{LA1,2}$ for the average molecular area for DIB and TTC within the monolayers, as ascertained at points A_1 and A_2, respectively, on the isotherms, were then computed using the formula $A_i(f) = (1-f)A_i(0\%) + f A_{LAi}$.

Sample	A_1	A_2	A_1/A_2	A_{LA1}	A_{LA2}
0 mol % (DPPC only)	79	46	1.7	0.0	0.0
9-mol % DIB	72	42	1.7	-2 ± 30	0.7 ± 30
16-mol % DIB	60	36	1.7	-40 ± 20	-20 ± 10
25-mol % DIB	58	34	1.7	-6 ± 9	-4 ± 8
9-mol % TTC	76	45	1.7	40 ± 30	30 ± 30
16-mol % TTC	79	47	1.7	80 ± 20	50 ± 10
25-mol % TTC	63	38	1.7	20 ± 9	10 ± 8

erside, CT) Minitrough, modified to mount on a Nikon Labophot 2A epifluorescence microscope (Tokyo, Japan). The trough itself was Teflon, and area compression was achieved using two hydrophillic Delrin barriers. The trough area was 7.5×25.5 cm^2 giving a surface area of 190 cm^2. The subphase volume was 0.10 l. Surface pressure measurements were made using a KSV Wilhelmy electrobalance with a platinum plate. To eliminate air convection and dust, the entire microscope was enclosed in a sealed plexiglass box, while the trough itself was enclosed in another sealed box. The temperature of the trough and its subphase was controlled using a water bath which circulated water through a heating block on the trough's base. Calibrated Teflon-coated thermistors were used to measure the temperature of the subphase and air. Temperatures were controlled to 21 °C $\pm$0.1 °C over the course of an isotherm, and subphase and air temperatures were equilibrated before each data-taking run.

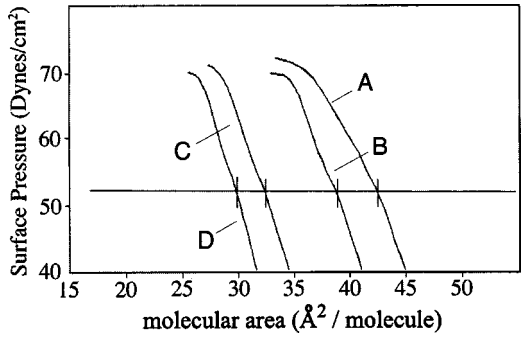

FIG. 3. Close-up of the surface pressure-molecular area isotherms for (right to left) 0-, 9-, 16-, and 25-mol % DIB: DPPC monolayers. At the LC to *S* phase transition, there is a change in the monolayer in-plane compressibility, indicated by a change in slope in the surface pressure-molecular area isotherm. In monolayers of DPPC containing either TTC or DIB, this change in slope decreases with increasing local anesthetic concentration, consistent with the local anesthetics being present as an impurity in the LC and *S* domains, rather than being excluded into the subphase at high in-plane densities.

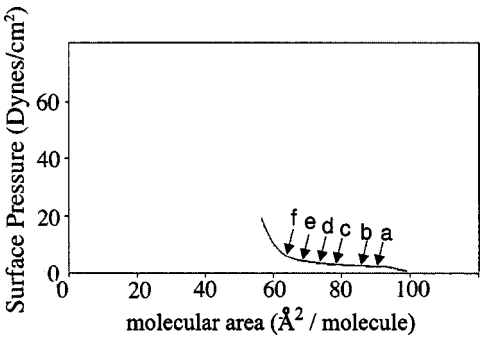

FIG. 4. Sample surface pressure vs molecular area (Å^2/molecule) isotherm for DPPC spread on the surface of a Langmuir trough, indicating typical points along the isotherm [(a)–(f)] at which epifluorescence images were collected for Figs. 5–10.

Clean water isotherms were performed before the monolayer studies began, yielding reproducibly low surface pressure increases of 0.1 dyn/cm or less on a 10:1 area compression. Both the trough and Wilhelmy plate were cleaned and extensively rinsed with ultrapure water in between samples with differing compositions. After spreading, films were allowed to equilibrate for 10 min before compression began. Compression times per isotherm were variable, ranging from 30-min continuous compressions to 2-h stepwise compressions for microscopy runs; either approach used compression rates which corresponded to 0.13 Å^2/molecule/sec for our trough area. Surface pressure-molecular area isotherms corresponding to stepwise compression during fluorescence microscopy runs were in good agreement with those taken in one shorter, continuous compression. For microscopy, approximate maximum and minimum molecular areas were roughly 115 and 50 Å^2.

For the epifluorescence measurements, samples were illuminated with a 100-W mercury lamp source filtered through a dichroic mirror/filter combination (Omega Optical, Brattleboro, VT). No photobleaching occurred because of a slight drift in domain position during the course of a typical measurement. A combination of a long working distance $40\times$ objective and a $5\times$ projection lens was used to give a field of view of $105\times135\ \mu$m^2. Images were collected using a Quantex (San Diego, CA) QC-100 image-intensified camera, and stored on VHS videotape. For quantitative analysis, individual images were digitized using a PCVisionPlus framegrabber from Imaging Technology (Bedford, MA) in a Pentium personal computer. The resulting eight bit 480 by 640-pixel images were analyzed using the MOCHA image processing package (Jandel Scientific, San Rafael, CA). For the purposes of quantitative analysis, images were first subjected to a 5×5-pixel median filter to average out noise, then clearfield corrected for nonuniform illumination. Inten-

sity thresholds were used to define the LC domains, and pixel counts were used to define the domain area A_D and perimeter P. The shape factor S, a measure of the compactness of a two-dimensional shape, was defined as $S = P^2/4\pi A_D$; a value of 1 corresponds to a perfect circle, while larger values indicate less compact shapes.

RESULTS AND DISCUSSION

Film-balance measurements

We obtained isotherms for LA (DIB or TTC):DPPC monolayers at concentrations of $f = 0$, 9, 16, and 25 mol % [Figs. 2(a) and 2(b)]. We observed the same general trend noted by earlier studies, in that the isotherms were progressively shifted to smaller molecular area with increasing LA concentration for either DIB or TTC; our quantitative results presented in Table I are also consistent with this earlier work [29]. Table I summarizes measurements of the molecular area at two points on each isotherm: A_1 corresponds to the onset of the LE-LC coexistence region, and A_2 is the point at which the surface pressure $\pi = 30$ dyn/cm. The constancy of the ratio A_1/A_2 for all samples is one indication of the fact that LA's only produce a rescaling of the average molecular area due to the inclusion of the DIB and TTC molecules in the monolayer. The shape of the isotherms is otherwise unperturbed.

The average in-plane molecular area for the local anesthetic molecules was computed from these data, assuming that the local anesthetics are entirely incorporated into the monolayer, and that DPPC molecules have the same molecular area in the local anesthetic samples as in the 0-mol % controls. The values of an $A_{\mathrm{LA1,2}}$ average molecular area for DIB and TTC within the monolayers, as ascertained at points A_1 and A_2, respectively, on the isotherms, were then computed using the formula $A_i(f) = (1-f)A_i(0\%) + f A_{\mathrm{LAi}}$. These results are included in Table I. The average in-plane molecular area for DIB was computed to be negative, which would correspond to a smaller in-plane molecular area for DPPC in these samples; however, within the large experimental uncertainties our results are consistent with zero average in-plane molecular area for DIB. This agrees with the interpretation that DIB inserts near the phospholipid headgroups; the average molecular area would be due then almost entirely to DPPC's two alkane chains. For TTC, the average in-plane molecular area is small but consistently positive, in keeping with expectations that TTC's chains may insert into the monolayer. The uncertainties in our data are too great to allow an accurate estimate of the exact TTC in-plane molecular area.

It also is clear from the isotherms that the LA molecules are incorporated within the monolayer in the LC phase even at high in-plane densities, rather than being excluded and squeezed out into the subphase altogether. Figure 3 shows the change in slope at low molecular area characteristic of the change in in-plane compressibility due to the transition between the LC and S phases of DPPC. As the concentration of LA (DIB or TTC) in the monolayer was increased, we observed a progressive rounding of this singularity in the slope of the surface pressure-molecular area isotherm at the LC-S phase transition (Fig. 3); this is consistent with what one would expect from the inclusion of an impurity (the LA) in the DPPC monolayer. If the TTC and DIB molecules were indeed excluded from the monolayer, this feature would be unaffected by changes in the LA concentration. This inclusion at high in-plane densities is consistent with earlier measurements of the subphase for evidence of intrinsic DIB fluorescence, which indicated that DIB does not get squeezed out [29].

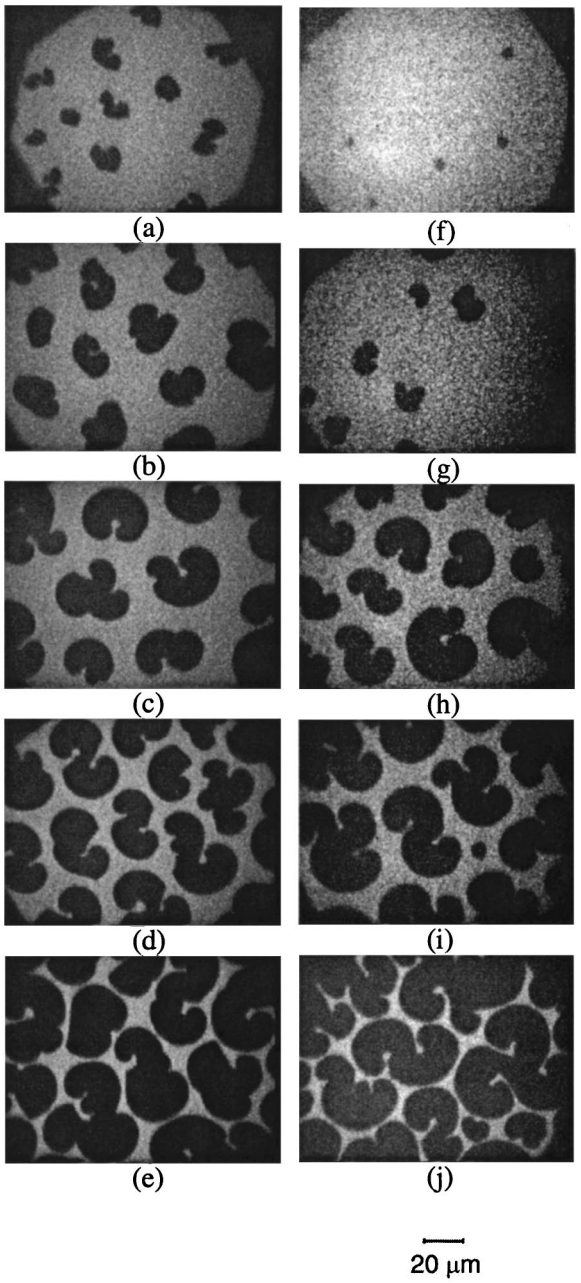

FIG. 5. Epifluorescence images of control DPPC monolayers containing no local anesthetic. The LC phase excludes the NBD-PC probe used, so LC domains appear black, while the surrounding LE phase contains probe and exhibits a high level of fluorescence. Similar results were seen for pH 6.0 [(a)–(e)] and pH 9.5 [(f)–(j)]. Values of pH, molecular area, and surface pressure corresponding to each image were for pH 6.0, respectively, (a) 85.9 Å^2, 2.5 dyn/cm; (b) 79.0 Å^2, 2.8 dyn/cm; (c) 73.4 Å^2, 3.3 dyn/cm; (d) 69.0 Å^2, 4.1 dyn/cm; and (e) 64.0 Å^2, 6.1 dyn/cm. For pH 9.5, they were (f) 83.6 Å^2, 6.4 dyn/cm; (g) 78.5 Å^2, 6.8 dyn/cm; (h) 72.5 Å^2, 7.5 dyn/cm; (i) 67.2 Å^2, 8.5 dyn/cm; and (j) 58.1 Å^2, 13.7 dyn/cm.

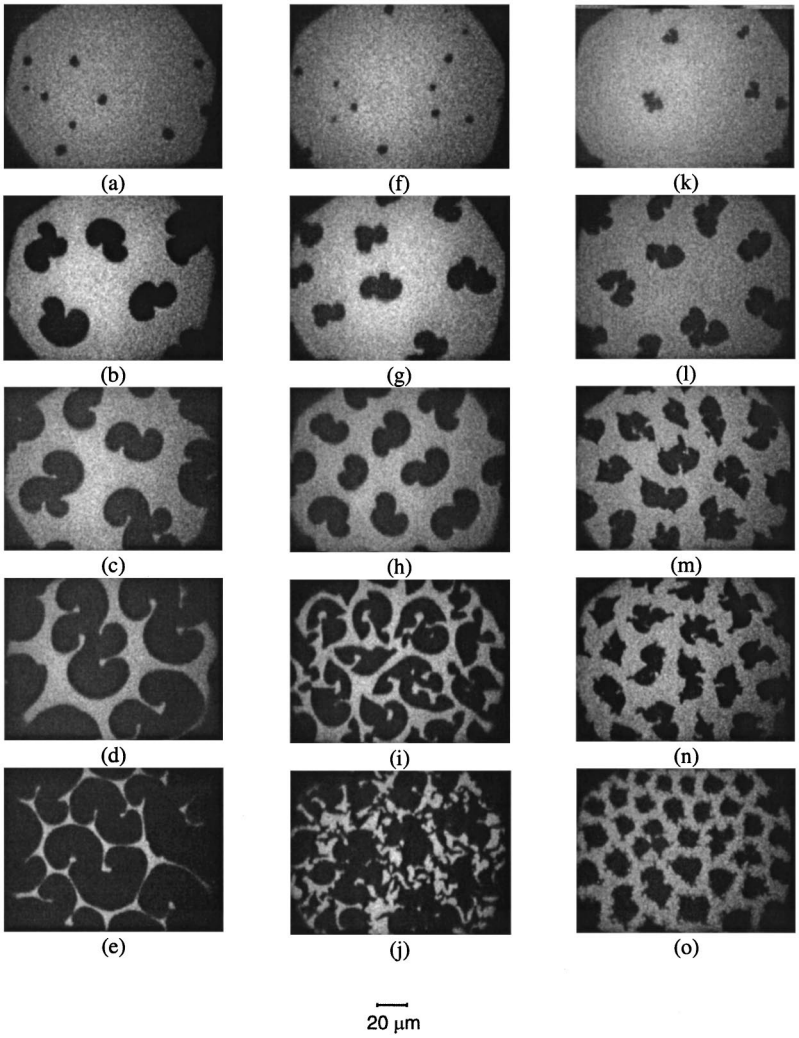

FIG. 6. Epifluorescence images for mixtures of DPPC with DIB at concentrations of 9 [(a)–(e)], 16 [(f)–(j)], and 25 [(k)–(o)] mol % at $p\mathrm{H}\ 6.0 \ll p\mathrm{K}_a$ for DIB. As is apparent in Figs. 6 and 7, at low pH the LC domains formed upon addition of either local anesthetic were consistently more highly ramified than those formed by DPPC controls only (Fig. 5). This effect became more pronounced with increasing DIB or TTC concentrations (see Fig. 7). Values of pH, molecular area, and surface pressure corresponding to each image at 9 mol % were (a) 72.5 Å^2, 5.7 dyn/cm; (b) 62.1 Å^2, 6.6 dyn/cm; (c) 57.3 Å^2, 7.1 dyn/cm; (d) 52.3 Å^2, 8.5 dyn/cm; and (e) 46.3 Å^2, 15.2 dyn/cm. Those at 16 mol % were (f) 59.1 Å^2, 5.9 dyn/cm; (g) 54.3 Å^2, 6.5 dyn/cm; (h) 48.9 Å^2, 7.2 dyn/cm; (i) 44.0 Å^2, 8.5 dyn/cm; and (j) 40.5 Å^2, 14.5 dyn/cm. Those at 25 mol % were (k) 60.2 Å^2, 5.9 dyn/cm; (l) 54.7 Å^2, 6.5 dyn/cm; (m) 50.6 Å^2, 7.1 dyn/cm; (n) 41.3 Å^2, 10.3 dyn/cm; and (o) 38.5 Å^2, 15.5 dyn/cm.

Epifluorescence microscopy

Epifluorescence microscopy was performed throughout the LE-LC coexistence region for mixed LA:DPPC and control DPPC-only monolayers at both pH 6.0 and 9.5. Figure 4 shows a typical isotherm, with arrows indicating the approximate points along the coexistence region at which the typical images in Figs. 5–8 were filmed. Images for LA:DPPC monolayers were expected to exhibit a larger fraction of LE vs LC phase for comparable points on the isotherms, relative to DPPC controls, due to the disordering effects of the LA. Since the LA was expected to partition preferentially into the less ordered LE phase, no effect on the LC domains was anticipated. However, the observed differences were more complex and subtle than the expectations. At pH 6.0, the LC domains observed for LA samples were substantially less compact and more ramified than those observed in control DPPC monolayers (Fig. 5). Similar effects were seen at low pH with both DIB (Fig. 6) and TTC (Fig. 7). Both the complexity of the LC domain shapes and the degree of monolayer uniformity varied reproducibly as the LA concentration increased over the range 0, 9, 16, and 25 mol % (Figs. 6 and 7). For both LA's, there was a clear dependence on concentration, with more dilute samples more closely resembling the controls. In DIB, differences from the controls were most noticeable in the 25-mol % LA samples, although they were still observable in the 16-mol % samples (Fig. 6). Monolayers containing TTC exhibited this effect more strongly than those containing DIB, and at lower concentrations, down to 9-mol % TTC (Fig. 6), correlating with the greater membrane solubility of TTC relative to DIB, and its greater anesthetic efficacy.

Figure 8 shows the results of a quantitative analysis of images for three of the samples shown in Figs. 5–7: DPPC only, 25% DIB, and 25% TTC. Although the analysis for only one isotherm for each sample is shown, images analyses were performed for three separate datasets for each sample to confirm reproducibility. In order to compare equivalent points on each isotherm, the results are plotted as a function of molecular area divided by A_1, the molecular area at the onset of the LC-LE coexistence region (Table I). These calculations showed quantitatively that neither the ratio of LC to LE phase [Fig. 8(a)] nor the average LC domain area [Fig. 8(b)] was affected by the presence of the LA. On the other hand, Fig. 8(c) shows an increase in the shape factor for 25% TTC and DIB samples relative to the DPPC-only controls over most of the isotherm; this provides a quantitative illustration of the observation that the LA-containing samples were notably less compact. The differences observed in the shapes of LC domains due to DIB or TTC incorporation were seen specifically over only a large fraction of the monolayer, and were not present uniformly over the entire monolayer; outside these regions, the monolayers were much

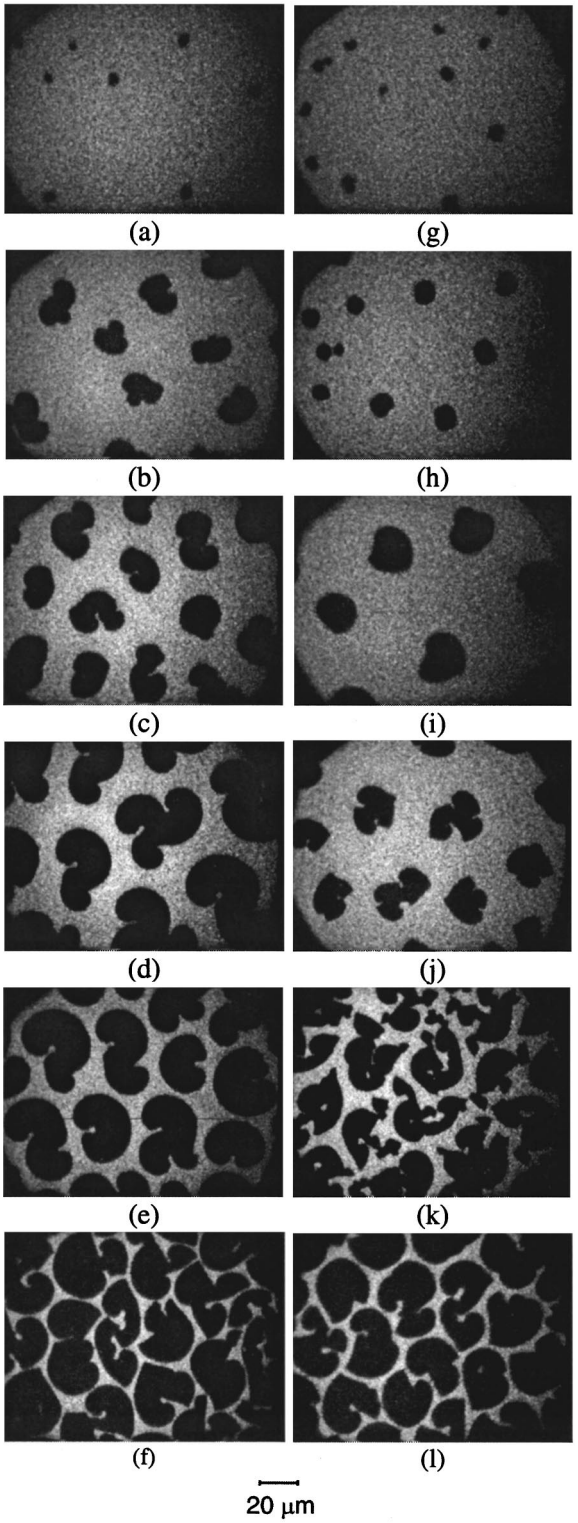

FIG. 7. Epifluorescence images for mixtures of DPPC with TTC at concentrations of 9 [(a)–(f)] and 25 [(g)–(l)] mol % taken at pH 6.0$\ll p$K$_a$ for TTC. Values of pH molecular area, and surface pressure corresponding to each image for 9-mol % TTC were (a) 80.8 Å^2, 4.4 dyn/cm; (b) 74.5 Å^2, 4.9 dyn/cm; (c) 69.4 Å^2, 5.2 dyn/cm; (d) 64.5 Å^2, 5.7 dyn/cm; (e) 59.8 Å^2, 6.6 dyn/cm; and (f) 59.9 Å^2, 9.1 dyn/cm. For 25-mol % TTC they were (g) 69.8 Å^2, 4.9 dyn/cm; (h) 65.4 Å^2, 5.8 dyn/cm; (i) 60.7 Å^2, 6.2 dyn/cm; (j) 55.2 Å^2, 6.8 dyn/cm; (k) 50.2 Å^2, 7.8 dyn/cm; and (l) 46.3 Å^2, 10.1 dyn/cm.

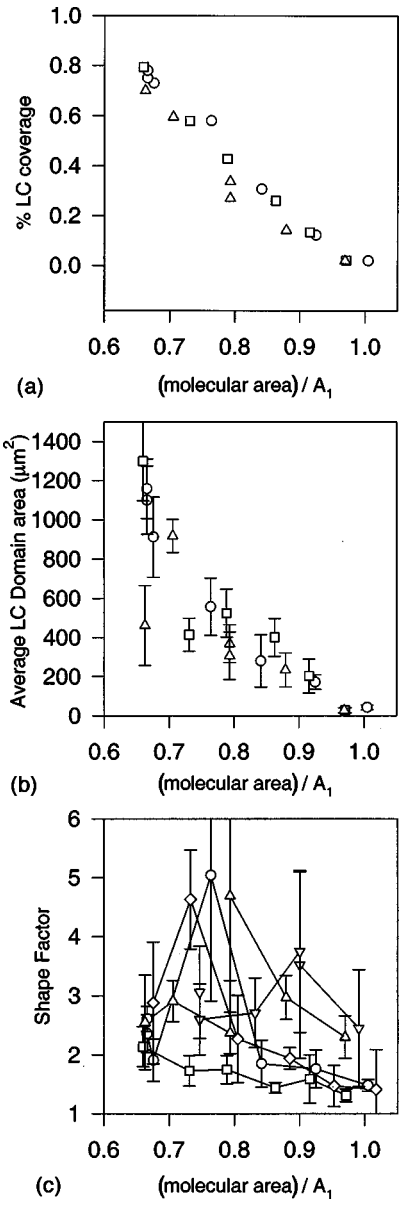

FIG. 8. Results of a quantitative analysis of the liquid condensed domains found in films containing either entirely DPPC (□), or DPPC:25-mol % DIB (△ and ▽) or 25-mol % TTC (○ and ◇) for pH 6.0. All data are shown plotted vs the molecular area divided by A_1, the molecular area at the onset of the LC-LE coexistence region (Table I); this ensures that equivalent points on each isotherm are being compared for different samples. A comparison of the variation of both (a) percent of LC domain coverage and (b) average LC domain area show no differences between the controls and LA-containing samples. (c) However, when the shape factor is computed for these samples, the 25% DIB and TTC samples are notably less compact over most of the isotherm. Two samples for each LA composition are plotted in (c) to show the variation in shape factor between samples.

closer in appearance to control DPPC samples. This is reflected in the wide spread in values of the shape factor in Fig. 8(c). The fraction of the monolayer which resembled the controls decreased as the concentration of the LA was increased. This suggests that the DIB or TTC molecules are localized primarily in specific regions of the monolayer during compression, rather than being uniformly distributed

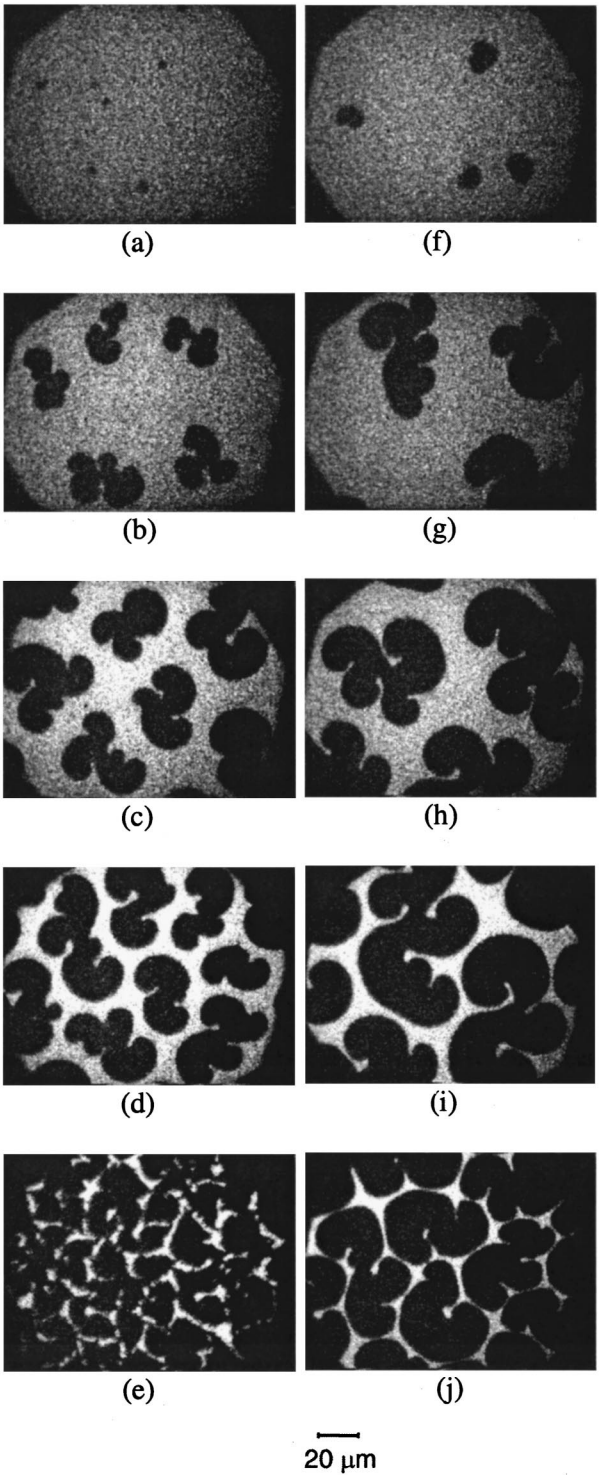

FIG. 9. Epifluorescence images for 25-mol % mixtures of DPPC with either (a)–(e) DIB or (f)–(j). TTC at pH 9.5$\gg p$K$_a$ of DIB and TTC. At these values of pH, both DIB and TTC should be uncharged. At high pH, mixed local anesthetic-DPPC monolayers resembled the control DPPC monolayers (Fig. 4). These results strongly suggest that the effect of DIB and TTC on in-plane molecular ordering depends upon electrostatic interactions. Values of pH, molecular area and surface pressure corresponding to each image for DIB were (a) 55.3 Å^2, 6.9 dyn/cm; (b) 50.7 Å^2, 7.3 dyn/cm; (c) 45.5 Å^2, 8.0 dyn/cm; (d) 40.2 Å^2, 9.9 dyn/cm; and (e) 36.1 Å^2, 17.9 dyn/cm. For TTC they were (f) 57.6 Å^2, 6.4 dyn/cm; (g) 52.7 Å^2, 6.8 dyn/cm; (h) 47.0 Å^2, 7.7 dyn/cm; (i) 42.4 Å^2, 9.9 dyn/cm; and (j) 38.5 Å^2, 16.5 dyn/cm.

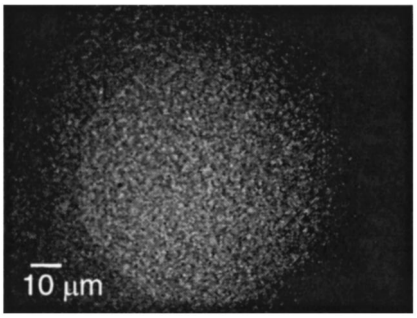

FIG. 10. Typical epifluorescence image taken using only DIB intrinsic fluorescence in the middle of the LC-LE coexistence region at pH 6.0. Compare with Fig. 5, in which NBD-PC is used as a probe which preferentially partitions into the LE phase. DIB fluorescence is distributed uniformly throughout the sample, indicating that DIB partitions into both LC (gel) and LE (fluid) phases.

over the entire monolayer.

The nature of the LC domains seen in these systems is very different than that seen in mixtures of DPPC with cholesterol [33], unsaturated phospholipid species or palmitic acid (unpublished results), indicating it is not simply a generic effect of introducing impurities into the monolayers. The compression rates used were adjusted to avoid purely kinetic effects due to rapid growth, such as fingering due to diffusion-limited aggregation [34].

The condensed domain shapes seen in DPPC monolayers containing DIB or TTC could be due to a variety of factors, including changes in the packing of nearest neighbors due to modified steric interactions, or to changes in the electric dipole-dipole interactions within the monolayers due to the presence of the cationic LA's. To probe the nature of these interactions, we performed epifluorescence microscopy on the 25-mol % DIB and TTC samples at high pH=9.5 to determine what aspects of the LA's effects are dependent on electrostatic interactions (see Fig. 9). At these values, the LA molecules should be electrically neutral. Control DPPC monolayers have identical LC domain shapes at both pH 6.0 and 9.5 (see Fig. 5). At pH 9.5, the 25-mol % DIB and TTC samples were very similar to the DPPC-only controls at all points across the LC-LE coexistence region. The 25-mol % DIB samples exhibited some of the distinctive faceting observed at low pH, but only at molecular area values consistent with the transition to the *S* phase. Specifically, for both LA's at pH=9.5, LC domains lacked the labyrinthine and distinctively faceted domain shapes characteristically observed in experiments run at low pH and high concentrations of anesthetic. This strongly suggests that the DIB and TTC molecules affect the LC domains primarily via altering the electric dipole-dipole interactions between DPPC molecules; this is consistent with this effect becoming insignificant at high pH, where either DIB or TTC are uncharged. The only residual effects observed for the high pH 25-mol % DIB samples were due to increased agglomeration of LC domains. This increase in the tendency of the domains to agglomerate at higher pH could be due to the fact that the DIB or TTC molecules' incorporation is decreasing the overall electrostatic repulsion between domains, an effect known to result in increased agglomeration [26]. This could result most simply from, e.g., the incorporation of TTC within the

monolayer decreasing the average in-plane electric dipole moment due to the inclusion of an electrically neutral molecule.

Intrinsic DIB fluorescence results

Using intrinsic DIB fluorescence, we attempted to determine the distribution of DIB within the monolayers at *p*H 6.0. Images were obtained across the LC-LE coexistence region for DPPC monolayers incorporating 5- and 25-mol % DIB, but no NBD-PC probe. (The lower DIB concentration was chosen to avoid self-quenching. We were unable to go to lower DIB concentrations because of limitations in the light levels available for imaging.) At both concentrations, LC domains were not observable when DIB was the only available fluorescent probe (Fig. 10). Instead, epifluorescence microscopy images obtained in these cases showed uniform levels of fluorescence, as confirmed by quantitative measurements of intensity profiles across the samples. To rule out the possibility that noise levels prevented us from seeing domains at the relatively low fluorescent intensity levels studied, we reproduced the intensity levels found with DIB only using low concentrations (0.004 mol %) of NBD-PC as a probe. Under these conditions, the preferential partitioning of NBD-PC into the LE phase still could be observed. We therefore conclude that DIB, unlike NBD-PC, partitions into both LC and LE phases. This finding is consistent with results from the isotherms showing that the transition pressures do not depend upon DIB concentration (Fig. 2), which indicates either complete phase separation or equal partitioning. If the DIB molecule is present in both the LC and LE phases, then its presence in the less fluid LC domains indicates that its effect on LC domain growth need not be limited to modifying the interface between the two phases.

To determine whether DIB is nonuniformly distributed throughout the plane of a monolayer on larger length scales, we measured the fluorescence intensity for a series of images taken at different points on the same monolayer at fixed molecular area. Variations in this intensity would indicate that the DIB concentration itself varies across the monolayer. The measured values of intensity were constant over the monolayer; however, we were limited in our ability to resolve small variations in in-plane DIB density because of the high background due to scattered light at these low light levels. As a result, we cannot directly correlate the nonuniform distribution of these domain shapes with a possible nonuniform DIB distribution.

CONCLUSIONS

These results lead to several conclusions for monolayer systems which may bear more generally on LA-membrane interactions. First, these results show no evidence of enhancement of ordered vs disordered phases in monolayers containing even high concentrations of DIB or TTC. In monolayers at least, these LA's do not appear to promote fluidity. In fact, isotherms recorded for DIB or TTC monolayers are identical when rescaled properly to account for this effect: no monolayer expansion is observed beyond the additional area due to the LA themselves. Indeed, it seems possible that DIB and TTC are present both within the LC and LE phases in phospholipid monolayers, rather than being localized to the gel-fluid interface or the less ordered phase. We also see no evidence for the exclusion of the LA from the monolayer, or its separation from the phospholipid in the monolayer. Thus, in monolayers at least, DIB and TTC affect membrane ordering as a whole, not just in isolated regions. Our average molecular area results are consistent with the hypothesis that TTC intercalates into the alkane chain region of the monolayer, but that DIB inserts only into the headgroup region.

On the other hand, it also seems clear that the LA's have a dramatic effect on promoting the formation of LC-LE interfaces, in agreement with calorimetry results for vesicles [19]. While our results have been obtained for high concentrations, this interfacial effect could extrapolate to shorter length scales for lower concentrations, which our optical techniques cannot probe. It seems especially suggestive that these effects were nonuniformly distributed over the monolayer, indicating that the LA may aggregate in the plane of the membrane, leading to locally enriched regions.

The results discussed above all relate to results obtained in a low *p*H regime, which should resemble the situation present at physiologically realistic values of *p*H. Our results for high *p*H point strongly toward the likelihood that the phospholipid-LA interaction does depend strongly on the charged state of both TTC and DIB. Taken as a whole, these observations support the idea that ''caine''-type LA's can alter the local interactions between phospholipids, potentially altering membrane order by disrupting the headgroup-headgroup electrostatic interactions. This could result in both modifications of the local packing of phospholipids and the promotion of longer interfaces between ordered and disordered phases. This effect of roughening interfaces within the membrane might influence the environment of membrane proteins, which presumably themselves exist at the boundary between more and less ordered regions of phospholipids.

ACKNOWLEDGMENTS

We wish to thank Benjamin North and Madison A. Compton for assistance with measurements on the controls. This work was supported in part by the National Science Foundation through Grant No. NSF-DMB-9109460, and in part through a grant from the Undergraduate Biological Sciences Education Initiative of the Howard Hughes Medical Institute, including support for Samuel D. Floyd through the Hughes Scholars Program.

[1] J. F. Butterworth IV and G. R. Strichartz, Anesthesiology **72**, 711 (1990); Anesthes. Analg. (Baltimore) **82**, 673 (1996).

[2] M. Akeson and D. W. Deamer, *Drug and Anesthetic Effects on Membrane Structure and Function* (Wiley-Liss, New York, 1991).

[3] Y. Kuroda, M. Ogawa, H. Nasu, M. Terashima, M. Kasahara, Y. Kiyama, M. Wakita, Y. Fujiwara, N. Fujii, and T. Nakagawa, Biophys. J. **71**, 1191 (1996).

[4] H. L. Li, A. Galue, L. Meadows, and D. S. Ragsdale, Mol. Pharmacol. **55**, 134 (1999).
[5] S. E. Ryan and J. E. Baenziger, Mol. Pharmacol. **55**, 348 (1999).
[6] M. Wood and A. J. J. Wood, *Pharmacology for Anesthesiologists* (Williams and Wilkins, Baltimore, 1990).
[7] I. Ueda, in *Drug and Anesthetic Effects on Membrane Structure and Function*, edited by R. C. Aloia, C. C. Curtain, and L. M. Gordon (Wiley-Liss, New York, 1991), pp. 15–43.
[8] J. R. Trudell, in *Drug and Anesthetic Effects on Membrane Structure and Function* (Ref. [7]), pp. 1–14.
[9] V. Luzzati, L. Mateu, G. Marquez, and M. Boro, J. Mol. Biol. **286**, 1389 (1999).
[10] H. Peters and F. Moll, Arnezeim.-Forsch. **45**, 1253 (1995).
[11] O. R. Hung, L. Comeau, M. R. Riley, S. Tan, S. Whynot, and M. Mezei, Can. J. Anaesth. **44**, 707 (1997).
[12] L. Langerman, G. J. Grant, M. Zakowski, E. Golomb, S. Ramanathan, and H. Turndorf, Anesth. Analg. (Baltimore) **75**, 900 (1992).
[13] C. Schwarz and W. Mehnert, J. Microencapsul. **16**, 205 (1999).
[14] R. Fisher, O. Hung, M. Mezei, and R. Stewart, Br. J. Anaesth. **81**, 972 (1998).
[15] C. Anteneodo, A. Rodahl, E. Meiering, M. L. Heynen, G. A. Sennisterra, and J. A. Lepock, Biochemistry **33**, 12 283 (1994).
[16] S. R. W. Louro, M. Tabak, and O. R. Nascimento, Biochim. Biophys. Acta **1190**, 319 (1994).
[17] Y. Kuroda and Y. Fujiwara, Biochim. Biophys. Acta **903**, 395 (1987).
[18] T. Shimooka, A. Shibata, and H. Terada, Biochim. Biophys. Acta **1104**, 261 (1992).
[19] W. W. Van Osdol, Q. Ye, M. L. Johnson, and R. L. Biltonen, Biophys. J. **63**, 1011 (1992).
[20] Y. Kuroda, M. Wakita, and T. Nakagawa, Chem. Pharm. Bull. (Tokyo) **42**, 2418 (1994).
[21] M. Boettner and A. Winter, Biophys. J. **65**, 2041 (1993).
[22] S. Maruyama, H. Matsuki, and S. Kaneshina, Prog. Anesth. Mech. **3**, 404 (1995).
[23] S. R. W. Louro, O. R. Nascimento, and M. Tabak, Biochim. Biophys. Acta **1189**, 243 (1994).
[24] S. R. W. Louro, C. Anteneodo, and E. Wajnberg, Biophys. Chem. **74**, 35 (1998).
[25] D. J. Keller, J. P. Korb, and H. M. McConnell, J. Phys. Chem. **91**, 6417 (1987).
[26] M. Flörsheimer and H. Möhwald, Chem. Phys. Lipids **49**, 231 (1989).
[27] A. Shibata, K. Ikawa, and H. Terada, Biophys. J. **69**, 470 (1995).
[28] H. Mozaffary, Thin Solid Films **244**, 878 (1994).
[29] A. Cavalli, G. Borissevitch, M. Tabak, and O. N. Oliveira, Jr., Thin Solid Films **284-285**, 731 (1996).
[30] A. Shibata, K. Ikawa, and H. Terada, Prog. Anesth. Mech. **3**, 374 (1995).
[31] K. Kjaer, J. Als-Nielsen, C. A. Helm, L. A. Laxhuber, and H. Mohwald, Phys. Rev. Lett. **58**, 2224 (1987).
[32] C. A. Helm, H. Mohwald, K. Kjaer, and J. Als-Nielsen, Biophys. J. **52**, 381 (1987).
[33] R. M. Weis and H. M. McConnell, J. Phys. Chem. **89**, 4453 (1985).
[34] A. Miller, W. Knoll, and H. Mohwald, Phys. Rev. Lett. **56**, 2633 (1986).